CapsuleNet for Micro-Expression Recognition

Nguyen Van Quang, Jinhee Chun, Takeshi Tokuyama
Graduate School of Information Sciences, Tohoku University, Sendai, Japan

***Abstract*— Facial micro-expression recognition has attracted researchers in terms of its objectiveness to reveal the true emotion of a person. However, the limited number of publicly available datasets on micro-expression and its low intensity of facial movements have posed a great challenge to training robust data-driven models for recognition task. In 2019, Facial Micro-Expression Grand Challenge combines three popular datasets, i.e. SMIC, CASME II, and SAMM into a single cross-database which requires the generalization of proposed method on a wider range of subject characteristics. In this paper, we propose a simple yet effective CapsuleNet for micro-expression recognition. The effectiveness of our proposed methods was evaluated on the cross-database micro-expression benchmark using the Leave-One-Object-Out cross-validation. The experiments show that our method achieved superiorly higher results than the baseline method (LBP-TOP) provided and other state-of-the-art CNN models.**

I. INTRODUCTION

A Micro-Expression (ME) is observed as a brief and involuntary facial movement when a person experiences an emotion but tries to hide their genuine underlying emotion. The normal facial expressions, also known as macro-expressions, last 1/2 to 4 seconds involving large areas of facial movements [9]. Meanwhile, Matsumoto and Hwang [10] suggest that micro-expressions occur in a fraction of a second (usually from 1/5 to 1/25 of a second) in small local areas. The brevity and low amplitude of facial movements make micro-expressions challenging to recognize in real-time by human eyes and even by experienced experts. Unlike macro-expressions, it is difficult for people to fake their micro-expressions. Therefore, micro-expressions play a crucial role in understanding human's underlying emotion, which powers various applications such as criminal interrogation [8], national security [5], and deceit detection [6], [7].

Due to the spontaneously induced characteristic of micro-expression, very few well-established datasets have been introduced, constraining the development of micro-expression research area. The number of samples in these datasets is usually too small to train robust micro-expression classifiers. In the second Micro-Expression Grand Challenge (MEGC), three spontaneous micro-expression datasets, including SAMM [2], CASME II [3], and SMIC [4], are integrated into a single cross-database with the motivation of increasing the number of samples as well as the diversity of subject characteristics. Although there have been no standard protocols of collecting and labeling the data, it is generally acceptable that MEs can be categorized into seven main emotions: happiness, surprise, contempt, anger, fear, sadness, and disgust. The previous MEGC challenge used the objective class labels following the proposal in [1]. However, the number of classes in the MEGC challenge is simplified into three labels, namely, negative, positive and surprise in order to reduce the ambiguity among datasets. The task of this MEGC challenge is to classify which of three categories an ME sequence belongs to with the ME cross-database.

Computational automatic analysis on micro-expression has recently attracted interest from researchers. Hand-crafted feature engineering methods were widely employed using from local binary pattern, histogram to optical flow as features to train traditional machine learning models [3], [14]–[20], [23]. Convolutional Neural Nework (CNN) gaining huge success on visual tasks were also applied successfully to ME recognition problem as feature extractors or classifiers [13], [24], [25]. The adoption of CNN networks replaces the manual feature engineering procedure by automatically finding a good feature representation for images. However, CNNs have still struggled to represents the part-whole relationships between the entity and and its parent in the image which is described to be powerful against spatial variations and adversarial attacks. To address the limitations of CNNs, Sabour et al. [29] quite recently introduced Capsule Networks (CapsuleNet), in which a capsule is a group of neurons that represent various properties of entities in a vector rather than a scalar. CapsuleNet find the part-whole relationships via an agreement routing mechanism. CapsuleNet have shown superiority over CNNs for digit [29] and object [30], [31] recognition.

Inspired by the recent success of capsule models on image recognition compared to traditional neural networks, we propose a CapsuleNet for micro-expression recognition using only apex frames. We would like to examine the capability of CapsuleNet to figure out the part-whole relationships and be trained effectively on only small datasets like micro-expression recognition task. The unweighted average recall score and unweighted F1 scores our model obtained in this challenge show that our method outperforms the provided LBP-TOP baseline method and the other state-of-the-art CNN models as well. In the full framework for ME recognition, we first apply the preprocessing step to detect unknown apex frames from frame sequences and extract the facial area from those apex frames. We, in turn, forward the cropped facial images into the CapsuleNet to perform classification. Our implementation for ME CapsuleNet is published at the github link: https://github.com/quangdtsc/megc2019. To the best of our knowledge, this is the first work which applies

978-1-7281-0089-0/19/$31.00

the idea of CapsuleNet on micro-expression recognition.

II. RELATED WORK

A. Hand-crafted approaches

Since the introduction of spontaneous ME datasets, several works were benefited from handcrafted feature engineering techniques such as Local Binary Pattern with three Orthogonal Planes (LBP-TOP) [20]. Yan et al. [3] utilized LBP-TOP to extract features, fitting into an SVM classifier to perform the recognition. Wang et al. [14] adopted LBP-Six Intersection Points (LBP-SIP) to refine the features. Li et al. [15] combined LBP-TOP, Histogram of Oriented Gradients, and Histogram of Image Gradient Orientation together, yielding single feature vectors to perform the recognition.

Besides, some techniques in video analysis were also adopted to capture the temporal information. X.Li et al. [16] used the Temporal Interpolation Model to sample uniformly the image frames from the ME sequence. Optical Flow techniques were also used as a good feature descriptor in several works. Shreve et al. [23] introduced an optical strain, the derivative of optical flow, as a feature descriptor which were used later in [17], [18]. Liu et al. [21] proposed Main Directional Mean Optical-flow (MDMO) to compute facial movements while Xu et al. [22] applied Facial Dynamics Map (FDM) and [19] used Bi-Weighted Oriented Optical Flow.

B. Deep learning approaches

Deep learning techniques have recently been applied to micro-expression recognition task. In their early work, Patel et al. [27] utilized Convolutional Neural Network (CNN) trained on macro-expression databases as a feature extractor. The extracted features are later forwarded to the genetic algorithm before fitting into traditional classifiers. Peng et al [25] proposed Dural Temporal Scale Convolutional Neural Network (DSTCNN) which was designed with shallow architecture to prevent overfitting on small micro-expression datasets. Very recently, Khor et al. [24] introduced an enriched version of Long-term Recurrent Convolutional Network which consists of spatial feature extractor and a temporal module to capture the temporal information. Peng et al. [13] applied transfer learning from macro-expression datasets to micro-expression recognition task on a ImageNet-pretrained ResNet10 model.

C. Capsule Networks

After the introduction of the CapsuleNet idea, more works have been done to examine the capability of CapsuleNet in various research areas. A CapsuleNet for brain tumor recognition designed by Afshar et al. [33] exceeds the performance of CNN networks. Jaiswal et al. [34] introduced Generative Adversarial Capsule Networks (CapsuleGAN) which outperforms CNN-based GAN at modeling image distribution on the MNIST dataset. For sentiment classification task in natural language processing, Wang et al. [32] proposed a RNN-Capsule architecture with state-of-the-art results.

These above works trigger the motivation for our work to examine whether we can apply successfully CapsuleNet to micro-expression recognition or not.

III. OUR PROPOSED METHOD

In this section, we present a complete framework for micro-expression recognition which adopts CapsuleNet architecture as the main component. The framework first detects and preprocesses the apex frames from the ME sequences if not provided before generating the ME predictions. We adopt transfer learning mechanism to initialize the pretrained weights on ImageNet for the first convolutional layers while training the network. Figure 1 summarizes the proposed framework with the preprocessing module and classification module.

A. Preprocessing

The ME sequence starts with an onset frame recording the neutral expression, and ends with an offset frame when the subject returns to the neutral expression. Meanwhile, the apex frame of ME sequence indicates the highest change in pixel intensities when the ME occurs. Several works [13], [19] show that apex frames provide rich information enough for ME recognition task. However, the apex frames are only annotated in SAMM and CASME II datasets while omitted in the SMIC dataset. In the preprocessing module, we first locate the apex frame of each ME, and segment the facial area out from the located apex frame.

We apply an open-source facial toolkit [1] to obtain 68 landmarks of the face in each frame of ME sequence. Following [28], we define 10 regions on the face based on the detected landmarks which represent for facial areas where muscle movements occur very frequently. The size of each cell is estimated by half of the mouth width heuristically. 10 regions were depicted in Figure 2.

To decide which one in the sequence is the apex frame, we compute the absolute pixel differences between the current frame with the onset and offset frames in the ten regions. To reduce the noise of environment, we normalize the summation of two difference by dividing it with the difference between the considered frame and its consecutive frame. Finally, we obtain the per-pixel average value for each frame in the ME sequence. The apex frame should indicate the peak of intensity differences with the onset and offset frame of the sequence. Therefore, we approximately select the frame with the highest per-pixel value of M_i. The variation of the mean of M_i is demonstrated in Figure 3.

$$f(\text{frame}_i, \text{frame}_j) = \frac{|\text{frame}_i - \text{frame}_j| + 1}{|\text{frame}_i - \text{frame}_{i\text{-}3}| + 1} \quad (1)$$

$$M_i = f(\text{frame}_i, \text{frame}_{onset}) + f(\text{frame}_i, \text{frame}_{offset}) \quad (2)$$

After detecting the apex frame (on SMIC dataset only), we crop the facial area on the apex frames of the ME sequences based on the facial landmarks, which later are fitted into the CapsuleNet for performing classification. We sumarize our preprocessing module in the Figure 4.

[1] https://github.com/ageitgey/face_recognition

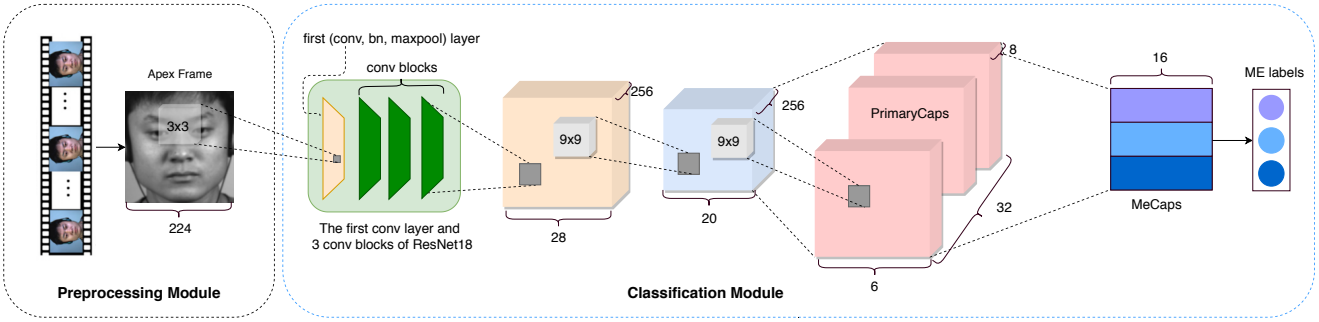

Fig. 1: The complete framework for micro-expression recognition using CapsuleNet architecture

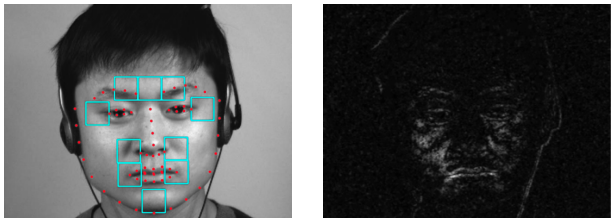

(a) 10 cells - Regions of Interest based on 68 facial landmarks.

(b) Frame differences for ME analysis.

Fig. 2: The demonstration for apex frame detection (example from CASME II)

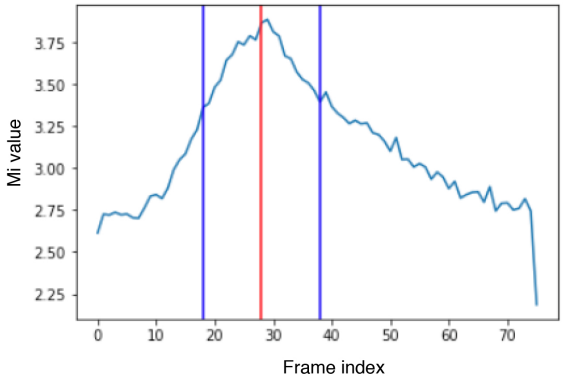

Fig. 3: The mean of M_i variation across an ME sequence. The ground truth labeling depicted in the ME sequence is marked with vertical red line.

B. CapsuleNet

We adopt CapsuleNet architecture, which aims to perform micro-expression recognition on the apex frame of its ME sequence. As illustrated in Figure 2, the architecture takes apex frames as input images. The cropped facial images of apex frames obtained are converted to color images and resized to the shape $[224, 224, 3]$. The input shape is extremely larger than the digit input shape in [29]. Since the facial movements of micro-expressions are low in intensity, we will lose a lot of information if we resize the input image into smaller shape. Therefore, we feed the input images into the first convolutional layer and three convolutional

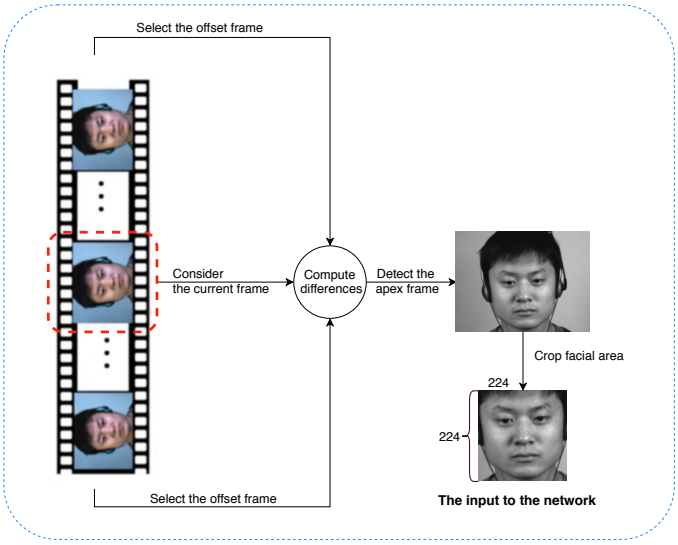

Fig. 4: The preprocessing module in our framework.

blocks of ResNet18 model [37] to transform pixel intensities into local features of shape $[28, 28, 256]$. We avoid to use larger ResNet versions like ResNet50 or ResNet101 to reduce the possibility of overfitting on small datasets. The initial weights of the model were set by the pretrained weights of ResNet18 respective layers on ImageNet. This design helps to reduce the exponential number of parameters while allows transferring the knowledge learned from object recognition on huge dataset like ImageNet.

These features, in turn, are passed into the primary capsule layer to obtain primary capsules (denoted as $PrimaryCaps$) by multiplying with convolutions. Each of primary capsule encapsulates the information and characteristics of an entity in a vector of neurons instead of a scalar value in CNNs. The activity of neurons in a capsule describes the instantiation parameters of that entity. We denote i as a capsule at the primary capsule layer and j as a capsule at the output capsule layer. The activation of the capsule j is determined based on the activations of all capsules in the primary layer. The coupling coefficient c_{ij} measures the agreement between capsule i and capsule j which is computed by routing softmax as follows:

$$c_{ij} = \frac{exp(b_{ij})}{\sum_k exp(b_{ik})} \tag{3}$$

where b_{ij} is denoted as the log probability of whether capsule i at primary capsule layer should be coupled with parent capsule j. b_{ij} is initially set to 0 and c_{ij} is iteratively refined via the dynamic routing process which we refer readers to [29] for more details. Then, input to capsule j (denoted as $\mathbf{x}_j$) is computed as follows:

$$\mathbf{x}_j = \sum_i c_{ij} \mathbf{W}_{ij} \mathbf{u}_i \tag{4}$$

In the output capsule, its length represents the probability that a certain entity exists while its orientation is forced to represents the properties of the entity. To ensure the length of the output vectors between the interval $[0, 1]$ while its orientation keep unchanged, a non-linearity **squash function** is applied. The final output of capsule j i.e. $\mathbf{v}_j$ is computed using the squash function as below:

$$\mathbf{v}_j = \frac{\|\mathbf{x}_j\|^2}{1 + \|\mathbf{x}_j\|^2} \frac{\mathbf{x}_j}{\|\mathbf{x}_j\|} \tag{5}$$

In our CapsuleNet, the output capsules (denoted as $MeCaps$) are used only for the purpose of micro-expression recognition but not for reconstruction of the input images. The additional subnet of reconstruction in [29] was added as a regularization for the overall network with input digit images of size $[28, 28]$. However, we remove this reconstruction part from the network since the input image size is much larger, $[224, 224]$, and the number of training dataset is quite small.

C. Network Optimization

We use the margin loss as an objective function for training our network:

$$L^{net} = \sum_k L_k^{margin} \tag{6}$$

where L_k^{margin} is the margin loss for the respective ME k. If an image contains an ME k, we force the length corresponding capsule to be long while we expect its length to be short when there is no ME in the image. To satisfy such conditions, we employ the following margin loss for each ME k:

$$\begin{aligned} L_k^{margin} =& T_k \max(0, m^+ - \|\mathbf{v}_k\|)^2 + \\ & \lambda_k (1 - T_k) \max(0, \|\mathbf{v}_k\| - m^-)^2 \end{aligned} \tag{7}$$

where $T_k = 1$ if ME k exists in the image and $T_k = 0$ if k does not exist in the image. λ_k specifies the effect of losses obtained when the ME is present or absent in the image. Finally, margin loss is provided to be zero if $\|\mathbf{v}_k\| > m^+$ when $T_k = 1$ and $\|\mathbf{v}_k\| < m^-$ when $T_k = 0$.

IV. EXPERIMENTS

A. Experimental setup

In our architecture, after passing input of size $[224, 224, 3]$ to the first convolutional block, we obtain a tensor of shape $[20, 20, 256]$. In the PrimCaps layer, we have 32 channels of convolutional 8D capsules where each capsule has 8 convolutional neuron units with a $[9 \times 9]$ kernel. Capsules in $[6 \times 6]$ grid share weights and we obtain $[6 \times 32]$ 8D capsule outputs. Each capsule in $PrimCaps$ is connected to each capsule in $MeCaps$ layer by a weight matrix $\mathbf{W}_{ij}$ of size $[16 \times 8]$. There are 3 capsules in the final outputs $MeCaps$. The margin loss L^{margin} is defined such that $m^+ = 0.9$, $m^- = 0.1$ and $\lambda_k = 0.5$ as suggested in [29]. During optimization we used Adam optimizer with a learning rate 0.0001 and decaying learning rate weight 0.9 in 20 epochs. We used 3 iterations of dynamic routing. The data augmentation was applied with some well-known transformations including: resizing, random cropping, mirroring, rotation and color jittering.

B. Baseline

A method from [12] using LBP-TOP was reimplemented as the first choice for the baseline for the MEGC challenge 2019. LBP-TOP descriptor first proposed by Zhao et al [20] is a well-known feature descriptor in micro-expression representation. In LBP-TOP method, frames in ME sequences were divided into $[5 \times 5]$ non-overlapping blocks with LBP-TOP parameters: radii $RXY, RXT, RYT = \{1, 1, 4\}$, number of neighboring points $P = 4$ for all planes, and $TIM = 10$.

We also compare our proposed model with two state-of-the-art network architectures for object recognition, namely, ResNet (ResNet18 version) [36] and VGG (VGG11 version) [37]. Two baseline models were modified by replaced the last fully connected layer with 1000 category outputs by another fully connected layer with 3 category outputs. Except for the last layer, the initial weights of the model were set by the pretrained weights on ImageNet. The multi-label cross entropy is employed as the loss function. The training procedure is performed with the same learning rate, epochs, and optimizers as training our proposed model.

C. Datasets

The cross-database of the 2019 challenge comprises of 3 popular spontaneous datasets as follows:

SMIC database [4] includes 164 micro-expressions from 16 subjects. Each ME was recorded at the speed of 100 fps and labeled with three general emotion labels: positive, negative and surprise. Recently, a new version of the database, SMIC-E, was published, which also contains some non-expression frames before and after the labeled micro-frames.

CASME II [3] is a comprehensive spontaneous micro-expression database containing 247 video samples, elicited from 26 Asian participants with an average age of 22.03 years old. The videos in this database showed a participant

evoked by one of five categories of micro-expressions: Happiness, Disgust, Repression, Surprise, Others.

SAMM, The Spontaneous Actions and Micro-Movements, [2] is a newer database of 159 micro-movements (one video for each) induced spontaneously from a demographically diverse group of 32 participants with a mean age of 33.24 years, and an even male-female gender split. Originally intended for investigating micro-facial movements, the SAMM was induced based on the 7 basic emotions.

Both the CASME II and SAMM databases have much in common: They are recorded at a high speed frame rate of 200 fps. Meanwhile, SMIC only record at the speed frame rate of 100 fps. To avoid the clutter and complication when combining all three datasets together, the challenge introduces a simplified class protocol for assigning labels for each sample as SMIC. There are altogether 68 subjects (16 from SMIC, 24 from CASME II, 28 from SAMM) after the databases are consolidated based on the new generic classes. Since the cross-database is too small to suffice the network, we enriched the datasets by acquiring the apex frame in ME sequence and its 4 neighbor frames as the training dataset. The resampling technique was also applied to reduce the effect of imbalance in the training dataset.

Dataset \ Class	Negative	Positive	Surprise	Total
SMIC	70	51	43	164
CASME II	88	32	25	145
SAMM	92	26	15	132
3DB-combined	250	109	83	442

TABLE I: The label summary on each dataset and cross-database (3DB-combined).

Evaluation metrics. Both Holdout-Database Evaluation (HDE) and Composite Database Evaluation (CDE) were used to evaluate the effectiveness of recognition methods in the last year MEGC challenge. However, HDE procedure is not a wise choice since it leads to combinatorial explosion of many permutations for train-test partitions from the cross-database. Following [12], we use Leave-One-Subject-Out (LOSO) cross-validation as a CDE method to report the performance on ME recognition. The real world situtation of people from a wide range of backgrounds including ethnicity, gender emotional sensitivities which were recorded in different settings would be considered with LOSO evaluation method. Furthermore, it also leads to subject-independent evaluation. Since the cross-database is apparently imbalanced, the recognition performance is evaluated with two balanced metrics:

Unweighted F1-score (UF1) is also commonly known as macro-averaged F1-score. We first calculate all the True Positives (TP_c), False Positives (FP_c) and False Negatives (FN_c) over all k folds of LOSO by each class c (of C classes), compute their respective F1-scores, and the final balanced F1-score is determined by averaging the per-class F1-scores as follows:

$$F1_c = \frac{2TP_c}{2TP_c + FP_c + FN_c} \tag{8}$$

$$\text{UF1} = \frac{1}{C}\sum_c F1_c \tag{9}$$

Unweighted Average Recall (UAR), or also known as balanced accuracy of the system. The per-class accuracy scores UAR_c are first calculated, and we average all Acc_c by the number of classes to obtain the final UAR score as below:

$$Acc_c = \frac{TP_c}{N_c} \tag{10}$$

$$\text{UAR} = \frac{1}{C}\sum_c Acc_c \tag{11}$$

Both UF1 and UAR give us a fair evaluation on how well the model performs on all the classes rather than biasing on only few certain classes.

V. Results and Discussion

We report the unweighted F1 and recall scores of our proposed model with the baseline provided by the challenge as well as the baselines we set up in Table II. Table II compares the UF1 and UAR scores on Full cross-database, and on separate parts including SMIC, CASME II and SAMM between the baselines and our proposed model. Our model obtained the UF1 score of 0.6512, and the UAR of 0.6498. Apparently, our model performance is the best among those of the baselines. The micro-expression performance of the proposed methods outperforms the state-of-the-art CNN networks, ResNet18 and VGG11 with large margins, approximately about 10%, which confirms the effectiveness of CapsuleNet architecture. Rather than using all the frames in ME sequence like LBP-TOP method to extract features, our model utilizes only a single apex frame of each ME as the input data. However, it still gained the 6.5% higher of UAR and UF1 compared with LBP-TOP method.

Figure 5 shows the LOSO confusion matrix of our proposed method. The recall rate of negative class is the highest (0.780) among the other classes since the negative samples are dominant in the cross-database. However, the recall rates of the two remaining classes are also acceptable with 0.596 and 0.575 respectively. This indicates the efficiency of the resampling technique for our CapsuleNet against imbalance-data effect.

Ablative study The additional layers added to the original CapsuleNet resolves the computational complexity. Although the choice of the additional layers could be quite diverse, we prefer the layers from state-of-the-art networks like ResNet and VGG to transfer the knowledge learned from bigger datasets like ImageNet with transfer learning technique. The layers extracted from ResNet18 are described as our proposed architecture above while the layers extracted from VGG11 are the first 3 convolutional layers of VGG11

Methods \ Cross-database	UF1 (Full)	UAR (Full)	UF1(SMIC)	UAR (SMIC)	UF1 (CASME II)	UAR (CASME II)	UF1 (SAMM)	UAR (SAMM)
LBP-TOP	0.5885	0.5791	0.2000	0.5280	0.7026	0.7429	0.3954	0.4102
VGG11	0.5264	0.5392	0.3461	0.3558	0.5315	0.5381	0.2871	0.4056
ResNet18	0.5392	0.5459	0.3576	0.3602	0.5367	0.5441	0.4821	0.4322
Our CapsuleNet	**0.6520**	**0.6506**	**0.5820**	**0.5877**	**0.7068**	**0.7018**	**0.6209**	**0.5989**

TABLE II: The LOSO cross-validation performances from our proposed methods and the baselines.

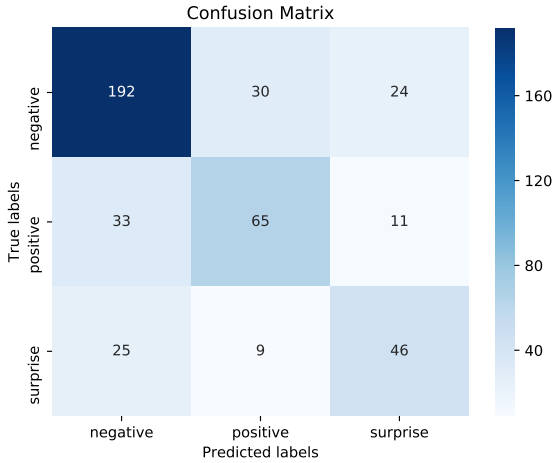

Fig. 5: Confusion matrix on cross-database with the LOSO cross-evaluation method. The number in each cell indicates the number of predictions.

accompanied by 3 respective max-pooling layers. The output feature shapes from both cases are the same at $[28, 28, 256]$. However, the Table III shows that the layers from ResNet18 used to extract features for CapsuleNet are the better choice than those of VGG11. The main reason is probably that the frequent use of max-pooling in VGG11 case has higher possibility to lose the spatial information CapsuleNet requires to learn than the use of convolutional layers with stride of 2 to reduce dimensionality in ResNet18 case.

Method \ Scores	Unweighted F1	Unweighted Average Recall
CapsuleNet used VGG11	0.6130	0.6260
CapsuleNet used ResNet18	0.6520	0.6506

TABLE III: The LOSO cross-validation performances for the ablative study.

VI. CONCLUSIONS

This work introduced a complete framework with a CapsuleNet for micro-expression recognition using only apex frames. The additional design is the key to reduce the computational complexity of the CapsuleNet and improve the generalization on small micro-expression datasets. Also, CapsuleNet exploits the knowledge from apex frames only without heavy and complicated computations when using all the frames in micro-expression sequence. Experimental results show the effectiveness proposed method which outperforms the LBP-TOP baseline and several powerful CNN models in micro-expression recognition.

VII. ACKNOWLEDGEMENTS

This work was supported by JSPS KAKENHI Grant Number 15H02665, 17K00002.

REFERENCES

[1] A. Davison, W. Merghani, and M.H. Yap, "Objective classes for microfacial expression recognition," Journal of Imaging, vol. 4, no. 10, p. 119, 2018.

[2] A. K. Davison, C. Lansley, N. Costen, K. Tan, and M. H. Yap, "Samm: A spontaneous micro-facial movement dataset," IEEE Transactions on Affective Computing, vol. 9, no. 1, pp. 116129, Jan 2018.

[3] W.-J. Yan, X. Li, S.-J. Wang, G. Zhao, Y.-J. Liu, Y.-H. Chen, and X. Fu, "Casme ii: An improved spontaneous micro-expression database and the baseline evaluation," PloS one, vol. 9, no. 1, 2014.

[4] Li X, Pfister T, Huang X, Zhao G, Pietika inen M (2013). "A Spontaneous Micro-expression Database: Inducement, Collection and Baseline," 10th Proc Int Conf Autom Face Gesture Recognit (FG2013). Shanghai, China. DOI: 10.1109/ FG.2013.6553717.

[5] Weinberger, S. (2010). "Airport security: intent to deceive?," Nature 412415. Doi: 10.1038/465412a.

[6] Ekman, Paul. (2009). "Lie catching and microexpressions," in The Philosophy of Deception, ed C. W. Martin (Oxford: Oxford University Press), 118133. Doi: 10.1093/acprof:oso/9780195327939.003.0008.

[7] Ekman, P. "Telling Lies: Clues to Deceit in the Marketplace, Politics, and Marriage," revised ed.; WW Norton Company: New York, NY, USA, 2009.

[8] Russell, T. A., Chu, E., and Phillips, M. L. (2006). "A pilot study to investigate the effectiveness of emotion recognition remediation in schizophrenia using the micro-expression training tool," Br. J. Clin. Psychol. 45, 579583. Doi: 10.1348/014466505X90866.

[9] Ekman, Paul. 2007. "Emotions Revealed: Recognizing Faces and Feelings to Improve Communication and Emotional Life," Macmillan.

[10] D. Matsumoto and H. S. Hwang, "Evidence for training the ability to read microexpressions of emotion," Motivation Emotion, vol. 35, pp. 181191, 2011.

[11] A. C. Le Ngo, R. C.-W. Phan, and J. See, "Spontaneous subtle expression recognition: Imbalanced databases and solutions," in Computer VisionACCV 2014. Springer, 2014, pp. 3348.

[12] Moi Hoon Yap, John See, Xiaopeng Hong, Su-Jing Wang. "Facial Micro-Expressions Grand Challenge 2018 Summary," In Automatic Face and Gesture Recognition (FG 2018), 2018 13th IEEE International Conference.

[13] Peng, M., Wu, Z., Zhang, Z., and Chen, T. (2018). "From Macro to Micro Expression Recognition: Deep Learning on Small Datasets Using Transfer Learning," In Automatic Face and Gesture Recognition (FG 2018), 2018 13th IEEE International Conference on (pp. 657-661).

[14] Y. Wang, J. See, C.W. Phan, et al. (2014). "LBP with Six Intersection Points: Reducing Redundant Information in LBP-TOP for Microexpression Recognition," Computer Vision–Asian Conference on Computer Vision. Springer International Publishing, 2123. Doi: 10.1007/978-3-319-16865-434.

[15] X. Li, X. Hong, A. Moilanen, et al. (2017). "Towards Reading Hidden Emotions: A Comparative Study of Spontaneous Micro-expression Spotting and Recognition Methods," IEEE Transactions on Affective Computing. Doi: 10.1109/TAFFC.2017.2667642.
[16] X. Li, T. Pfister, X. Huang, G. Zhao, and M. Pietikainen, "A spontaneous micro-expression database: Inducement, collection and baseline," in IEEE FG, 2013, pp. 16.
[17] S.-T. Liong, J. See, R. C.-W. Phan, A. C. Le Ngo, Y.-H. Oh, and K. Wong, "Subtle expression recognition using optical strain weighted features," in ACCV. Springer, 2014, pp. 644657.
[18] S.-T. Liong, J. See, R. C.-W. Phan, Y.-H. Oh, A. C. Le Ngo, K. Wong, and S.-W. Tan, "Spontaneous subtle expression detection and recognition based on facial strain," Signal Processing: Image Communication, vol. 47, pp. 170182, 2016.
[19] S.-T. Liong, J. See, R. C.-W. Phan, and K. Wong, "Less is more: Micro-expression recognition from video using apex frame," arXiv preprint arXiv:1606.01721, 2016.
[20] G. Zhao and M. Pietikainen, "Dynamic texture recognition using local binary patterns with an application to facial expressions," IEEE Trans. on PAMI, vol. 29, no. 6, pp. 915-928, 2007.
[21] Y. J. Liu, J. K. Zhang, W. J. Yan, et al, "A Main Directional Mean Optical Flow Feature for Spontaneous Micro-Expression Recognition," 7(4):299-310.
[22] F. Xu, J. Zhang, J. Wang, "Micro-expression Identification and Categorization using a Facial Dynamics Map," IEEE Transactions on Affective Computing, 2017, 8(2): 254-267.
[23] M. Shreve, S. Godavarthy, D. Goldgof, and S. Sarkar, "Macroand micro-expression spotting in long videos using spatiotemporal strain," in IEEE FG, 2011, pp. 5156.
[24] Khor, Huai-Qian and See, John and Phan, Raphael CW and Lin, Weiyao, "Enriched Long-term Recurrent Convolutional Network for Facial Micro-Expression Recognition," In Automatic Face and Gesture Recognition (FG 2018), 2018 13th IEEE International Conference.
[25] M. Peng, C. Wang, T. Chen, et al, "Dual Temporal Scale Convolutional Neural Network for Micro-Expression Recognition," Frontiers in Psychology, 2017, 8:1745.
[26] D. H. Kim, W. J. Baddar, and Y. M. Ro, "Micro-expression recognition with expression-state constrained spatio-temporal feature representations," in Proc. of the ACM MM. ACM, 2016, pp. 382386.
[27] D. Patel, X. Hong, and G. Zhao, Selective Deep Features for Micro-Expression Recognition, 23rd International Conference on Pattern Recognition, 2016:2258-2263.
[28] Diana Borza, Radu Danescu, Razvan Itu, and Adrian Sergiu Darabant, "High-Speed Video System for Micro-Expression Detection and Recognition," In Sensors 2017, 17, 2913, DOI:10.3390/s17122913.
[29] Sara Sabour, Nicholas Frosst, and Geoffrey E Hinton. "Dynamic routing between capsules," In Advances in Neural Information Processing Systems, pages 38593869, 2017.
[30] E. Xi, S. Bing, and Y. Jin. "Capsule network performance on complex data," arXiv preprint arXiv:1712.03480, 2017.
[31] G. Hinton, N. Frosst, and S. Sabour. "Matrix capsules with em routing," in ICLR 2018.
[32] Y. Wang, A. Sun, J. Han, Y. Liu, and X. Zhu. "Sentiment analysis by capsules," 2018.
[33] P. Afshar, A. Mohammadi, and K. N. Plataniotis. Brain tumor type classification via capsule networks. arXiv preprint arXiv:1802.10200, 2018.
[34] A. Jaiswal, W. AbdAlmageed, and P. Natarajan. "Capsule-gan: Generative adversarial capsule network," arXiv preprint arXiv:1802.06167, 2018.
[35] Itir Onal Ertugrul, Laszlo A. Jeni, Jeffrey F. Cohn, "FACSCaps: Pose-Independent Facial Action Coding With Capsules," In The IEEE Conference on Computer Vision and Pattern Recognition (CVPR) Workshops, 2018, pp. 2130-2139.
[36] Kaiming He and Xiangyu Zhang and Shaoqing Ren and Jian Sun. "Deep Residual Learning for Image Recognition," arXiv preprint arXiv:1512.03385, 2015.
[37] Karen Simonyan, Andrew Zisserman, "Very Deep Convolutional Networks for Large-Scale Image Recognition," ArXiv preprint arXiv:1512.03385, 2014.